

# In-situ micro frequency dependent electric field sensors to verify model predictions of cure and aging

Justin Doo · Yuemei Zhang · Judd Compton ·  
David Kranbuehl · Alfred C. Loos

Published online: 8 August 2006  
© Springer Science+Business Media, LLC 2006

**Abstract** Frequency dependent electric field measurements using in situ micro sensors, FDEMS, is a particularly useful technique for monitoring the changing state of a polymer in a composite (or in an adhesive joint or as a coating) during fabrication and aging during use in the field. Measurements can be made in the laboratory to monitor the polymerization process and to monitor durability and aging in an environmental chamber or other degradative environment. Equally important, the FDEMS in situ micro sensor monitoring technique can be used to monitor cure in production ovens and autoclaves on the plant floor as well as outside, for example, coatings on the surface of a ship in dry dock. Durability and aging can be monitored while the object is in use. Examples are a marine coating on a ship, the protective coating on the liner of an acid containing tank, a rocket propellant, an adhesive in a bond joint, or the polymer in a composite structure.

## Introduction

Frequency dependent electric field measurements using in situ micro sensors, FDEMS, is a particularly useful technique for monitoring the changing state of a polymer in a composite (or in an adhesive joint or as a coating) during fabrication and aging during use in the field [1–5].

---

J. Doo · Y. Zhang · J. Compton · D. Kranbuehl (✉)  
Chemistry and Applied Science Departments, College  
of William and Mary, Williamsburg, VA 23187, USA  
e-mail: dekran@wm.edu

A. C. Loos  
Department of Chemical Engineering, Michigan State  
University, East Lansing, MI 48824, USA

Measurements can be made in the laboratory to monitor the polymerization process and to monitor durability and aging in an environmental chamber or other degradative environment. Equally important, the FDEMS in situ micro-sensor monitoring technique can be used to monitor cure in production ovens and autoclaves on the plant floor as well as outside, for example, coatings on the surface of a ship in dry dock. Durability and aging can be monitored while the object is in use. Examples are a marine coating on a ship, the protective coating on the liner of an acid containing tank, a rocket propellant, an adhesive in a bond joint, or the polymer in a composite structure.

The FDEMS micro sensing technique ought to be more widely used, particularly in monitoring cure and aging. One reason the planar micro sensor should be used more extensively is that it is ideally suited to monitoring changes in state at a particular position or ply layer in a complex composite structure. This condition is difficult to duplicate in most rheological and calorimetric measurements. Furthermore, unlike some optical and calorimetric techniques, the sensitivity does not decrease when one tries to detect changes during the late stages of cure. Remote, planar, micro electric field sensors provide simple, in situ, accurate measurements of changes in state throughout the fabrication process and with a high degree of sensitivity.

A probable reason why FDEMS is not used more widely is that there is a limited understanding by practitioners in industry of the physical principles upon which the instrumental technique is based. Often there is a desire to cut short the importance of understanding the science behind the frequency dependence of electric measurements and to simply interpret changes in the state of the instrument's signal. This simplified approach leads to misinterpretation and error.

The key to successfully using electric field sensor measurements to monitor changes in the state of a resin

system during cure and aging in the use environment, is to understand the frequency dependence of the complex permittivity  $\epsilon^*$ , a force–displacement parameter similar to the complex modulus  $G^*$  or compliance  $J^*$  in rheological measurements.

One might ask why do one need in situ microsensors in addition to accurate composite models for fabrication. Modeling and individual thinking that lead to a procedure-driven cure cycle are beset with operating difficulties. Most notably, as has been described by George Springer (6), modeling requires extensive material data characterization of resin properties, as well as fabric and tooling properties that are time consuming to measure and, most importantly, that will vary from day to day, batch, and lay up to lay up.

This report will describe the use of FDEMS micro sensors to monitor the changes in processing properties and buildup in use properties of an epoxy resin as a function of ply depth in the autoclave mold during cure of a 1 inch thick graphite composite and of use this data to verify a process model. It will also discuss monitoring the fabrication process during resin infiltration and cure of an advanced fiber architecture composite and to verify model predictions of that fabrication process. Use of the sensor to monitor cure using UV or e-beam radiation will be described. Use of the sensor output to intelligently control the fabrication process of a composite in conjunction with model predications will also be described.

Then the application of FDEMS sensor to monitor ingress of degradative components into a coating, an adhesive bond line, and a composite structure during use for the purpose of life monitoring and evaluating the time for replacement will be briefly discussed.

## Instrumentation

Frequency dependent complex dielectric measurements are made by using an impedance analyzer controlled by a microcomputer (1,2). In the work discussed here, measurements at frequencies from 5 Hz to  $5 \times 10^6$  Hz are taken continuously throughout the entire cure process at regular intervals and converted to the complex permittivity,  $\epsilon^* = \epsilon' - i\epsilon''$ . The measurements are made with a geometry independent planar interdigitated microsensor. This system is used with either a Hewlett Packard or a Schlumberger impedance bridge. The system permits multiplexed measurement of several sensors. The sensor itself is planar, 1 by 1/2 in. in area and 3-mm thick. This single sensor-bridge microcomputer assembly is able to make continuous uninterrupted measurements of both  $\epsilon'$  and  $\epsilon''$  over 10 decades in magnitude at all frequencies. The sensor is inert and has been used at temperatures exceeding 400 °C and pressures over 1000 psi.

## Theory

Frequency dependent measurements of the dielectric impedance of a material as characterized by its equivalent capacitance,  $C$ , and conductance,  $G$ , are used to calculate the complex permittivity,  $\epsilon^* = \epsilon' - i\epsilon''$ , where  $i$  is the imaginary number,  $\omega = 2\pi f$ ,  $f$  is the measurement frequency, and  $C_0$  is the equivalent air replacement capacitance of the sensor.

$$\begin{aligned}\epsilon'(\omega) &= \frac{C(\omega)\text{material}}{C_0} \\ \epsilon''(\omega) &= \frac{G(\omega)\text{material}}{C_0}\end{aligned}\quad (1)$$

This calculation is possible when using the sensor whose geometry is invariant over all measurement conditions. Both the real and the imaginary parts of  $\epsilon^*$  can have dipolar (d) and ionic (i)-charge polarization components.

$$\begin{aligned}\epsilon' &= \epsilon'_d + \epsilon'_i \\ \epsilon'' &= \epsilon''_d + \epsilon''_i\end{aligned}\quad (2)$$

Plots of the product of frequency ( $\omega$ ) multiplied by the imaginary component of the complex permittivity  $\epsilon''(\omega)$  make it relatively easy to visually determine the  $\epsilon''(\omega)$  permittivity when the low frequency magnitude of  $\epsilon''$  is dominated by the mobility of ions in the resin and when at higher frequencies the rotational mobility of bound charge dominates  $\epsilon''$ . Generally, the magnitude of the low frequency overlapping values of  $\omega\epsilon''(\omega)$  can be used to measure the change with time of the ionic mobility through the parameter  $\sigma$  where

$$\begin{aligned}\sigma(\text{ohm}^{-1}\text{cm}^{-1}) &= \epsilon_0\omega\epsilon''_i(\omega) \\ \epsilon_0 &= 8.854 \times 10^{-14} \text{C}^2 \text{J}^{-1} \text{cm}^{-1}\end{aligned}\quad (3)$$

The changing value of the ionic mobility is a molecular probe that can be used to quantitatively monitor the viscosity of the resin during cure. The dipolar component of the loss at higher frequencies can then be determined by subtracting the ionic component.

$$\epsilon''(\omega)(\text{dipolar}) = \epsilon''(\omega) - \frac{\sigma}{\omega\epsilon_0}\quad (4)$$

The peaks in  $\epsilon''(\text{dipolar})$  (which are usually close to the peaks in  $\epsilon''$ ) can be used to determine the time or point in the cure process when the *mean* dipolar relaxation time,  $\tau$ , has attained a specific value  $\tau=1/\omega$ , where  $\omega=2\pi f$  is the frequency of measurement. The dipolar mobility as measured by the mean relaxation time  $\tau$  can be used as a molecular probe of the buildup in  $T_g$ . The time occurrence of a given dipolar relaxation time as measured by a peak in a

particular high frequency value of  $\epsilon''(\omega)$  can be quantitatively related to the attainment of a specific value of the resin's  $T_g$ . Finally, the tail of the dipolar relaxation peak as monitored by the changing value of  $(d\epsilon''/dt)/\epsilon''$  can be used for in situ monitoring during processing the buildup in degree of cure and related end-use properties such as modulus, hardness, etc., during the final stages of cure or post cure.

**Isothermal cure**

The variation in the magnitude of  $\epsilon''$  with frequency and with time for the diglycidylether Bisphenol-A amine epoxy held at 121 °C is shown in Fig. 1. The magnitude of  $\epsilon''$  changes four orders of magnitude during the course of the polymerization reaction. A plot of  $\omega \epsilon''$  is a particularly informative representation of the polarization process because as discussed from Eqs. (1) to (4), overlap of  $\omega \epsilon''(\omega)$  frequency for differing frequencies indicates when and at what time translational diffusion of charge, which can be used to monitor viscosity and reaction advancement, is the dominant physical process affecting the loss. Similarly, the peaks in  $\omega \epsilon''(\omega)$  for individual frequencies indicate the dipolar rotational diffusion relaxation time, a quantity which can be used to monitor  $T_g$ .

The frequency dependence of loss  $\epsilon''$  is used to find  $\sigma$  by determining from a computer analysis, or a log–log plot of  $\epsilon''$  versus frequency, the frequency region where  $\omega \epsilon''(\omega)$  is a constant. In this frequency region the value of  $\sigma$  is determined from Eq. (3).

Figure 2 is a plot of  $\log(\sigma)$  versus  $\log(\text{viscosity } [\eta])$  constructed from dielectric data and measurements on a dynamic rheometer. The figure shows that at a viscosity less than 1 Pa s, (10 P),  $\sigma$  is proportioned to  $1/\eta$  because the slope of  $\log(\sigma)$  versus  $\log(\eta)$  is approximately  $-1$ . The gel point of the polymerization reaction occurs at 90 min

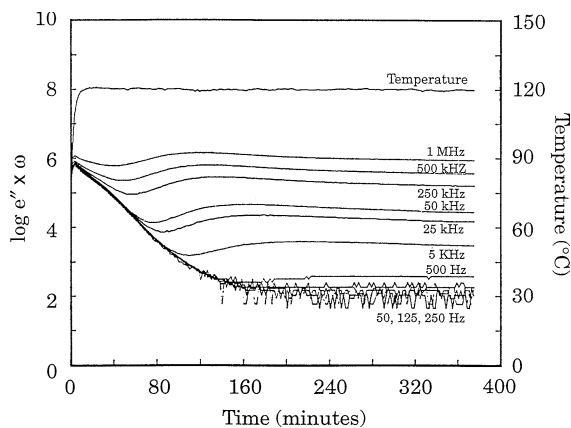


**Fig. 1** The dielectric loss multiplied by frequency versus time over a range of frequencies during cure of an epoxide at 120 °C

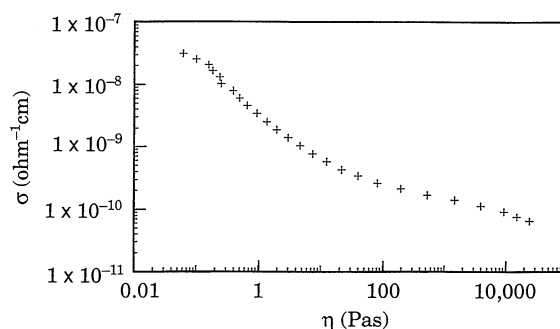


**Fig. 2** The correlation of changes in the specific conductivity with the viscosity during cure of an epoxide

based on the crossover of  $G'$  and  $G''$  measured at 40 rad/s. This result is very close to the time at which  $\eta$  achieves 100 Pa s, which is also often associated with gel. The region of gel marks the onset of a much more rapid change in viscosity than with  $\sigma$ . This change is undoubtedly because as gel occurs the viscoelastic properties of the resin involve the cooperative motion of many chains while the translational diffusion of the ions continues to involve motions over much smaller molecular dimensions.

The time of occurrence of a characteristic dipolar relaxation time can be determined by noting the time at which  $\epsilon''_{\text{dipolar}}$  achieves a maximum for each of the frequencies measured where  $\tau = 1/2\pi f$  at the time at which  $\epsilon''_{\text{dipolar}}$  achieved a maximum for frequency,  $f$ . Values of  $\tau$  can be measured over a range of frequencies and temperatures. The time of occurrence of a given peak in  $\epsilon''$  and the corresponding  $\tau$  is directly related to the time of achievement of a specific degree of reaction and the value of  $T_g$  at that point in time. This relationship between the peak in  $\epsilon''$  at each frequency and degree of cure and  $T_g$  is made in the laboratory in conjunction usually with differential scanning calorimetry measurements versus time at the same temperature.

Figure 3 is a plot showing the correlation of  $\sigma$  measured with the electric field sensors versus degree of cure  $\alpha$  as determined by differential scanning calorimetry measurements at identical times during a 120 °C cure. Figure 4 demonstrates how the change in  $d\epsilon''/dt$  can detect the final

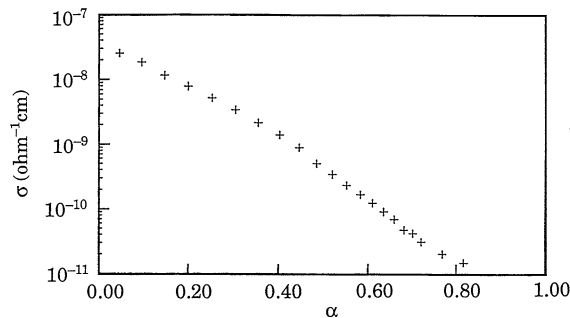


**Fig. 3** The correlation of changes in the specific conductivity with the reaction advancement during cure of an epoxide

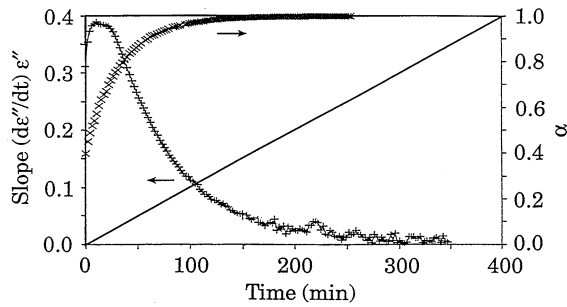


**Fig. 4** The correlation of changes in the rate of change of the dielectric loss with changes in the reaction advancement near the end of cure of an epoxide

buildup in full cure as  $\alpha$  approaches 1.0 with considerably more precision than a DSC measurement.

In summary, these in situ sensing measurements of  $\epsilon''$ ,  $\sigma \frac{d\epsilon''}{dt}$  and peaks in  $\epsilon''(\omega)$  can be used to monitor changes in essential cure processing properties, viscosity, degree of cure and buildup in  $T_g$ , during fabrication at any point in the production mold.

**Monitoring the cure process in the mold**

**Thick laminates**

Figure 5 is a plot of the sensors output during a typical epoxy cure cycle in the mold [7, 8]. Here, the temperature both lags behind and overshoots the expected hold temperature due to the mass and heat transfer characteristics of a particular oven, autoclave and mold. Yet, using the correlation relations developed in Figs. 2–4 for a particular resin, the sensor output in Fig. 5 can be used to monitor the actual state, changing viscosity, degree of cure and  $T_g$  at a particular position in the composite laminate.

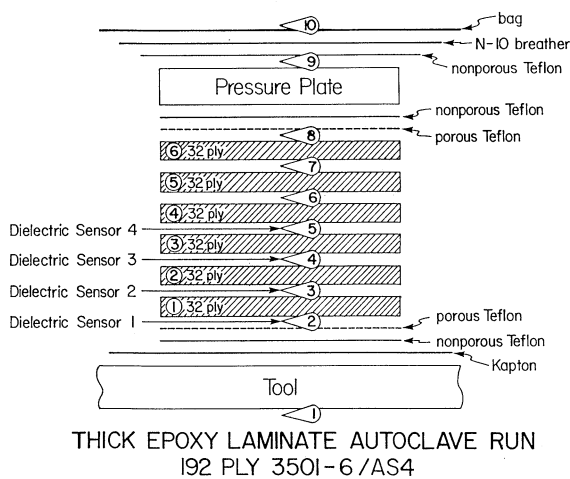


**Fig. 5** Positions of the sensors in a thick 192 ply epoxy laminate

Figures 6 and 7 display the positions of sensors in a one inch thick 192 ply epoxy-photo graphite laminate.

Figure 8 shows the sensor monitored viscosity. Here it is evident how the viscosity in the center lags behind the



**Fig. 6** A photograph of the thick 192 ply epoxy laminate with the embedded sensors after cure

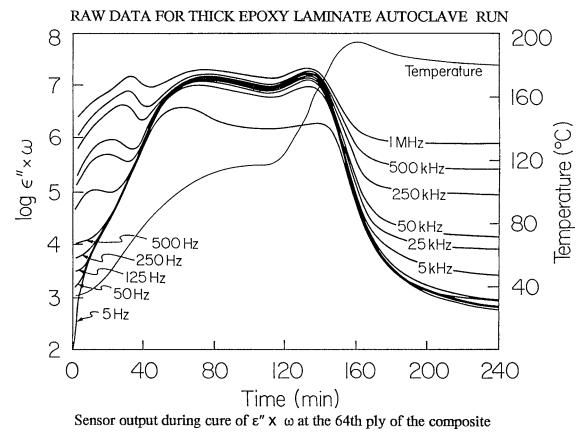


**Fig. 7** The dielectric loss multiplied by frequency versus time over a range of frequencies during cure of a 192 ply thick epoxy laminate at the 64th ply in an autoclave

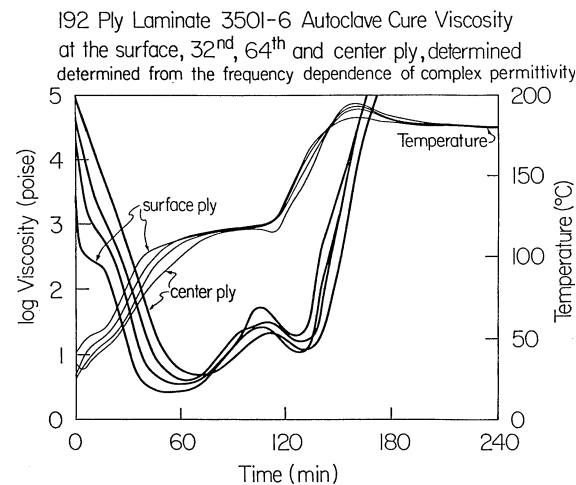


**Fig. 8** The sensor measured viscosity at each sensor ply location during cure in the autoclave

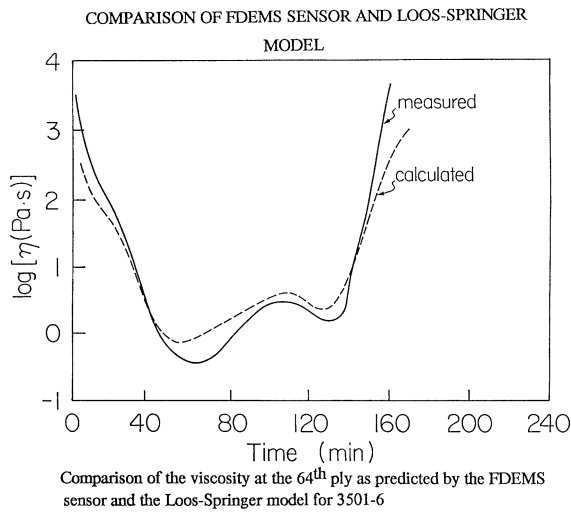


**Fig. 9** The comparison of the sensor measured viscosity at the 64th ply versus the predictions of the Springer-Loos model

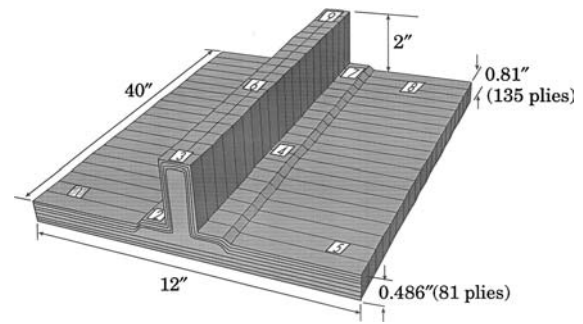
viscosity at the surface until the ramp approaching the final hold temperature. At about 130 minutes the viscosity at the center ply catches up with the outside ply and a minimum similar viscosity is achieved at the same time uniformly throughout all 192 plies. This is a key final time for pressure consolidation of the 192 ply laminate. The fact that all plies achieve the same viscosity at the same time is undoubtedly one reason why this time-temperature cure cycle developed by trial and error is successful in creating a well formed final product.

Figure 9 shows how this sensor output can be used to verify model predictions such as from the Loos-Springer process model, during fabrication on the plant floor [6–8].

**Resin infusion of 3-dimensionally advanced fiber architecture preforms**

This is the second application where we have used electric field sensors to verify model predictions and monitor the processing properties as a function of position. Figure 10 is a diagram of a blade stiffened panel which is a prototype for a wing. Here resin is placed below the panel. Then temperature is used to reduce the viscosity of the epoxy and a vacuum to draw the resin up into the panel. Sensors 2 through 9 were placed on top of the panel to monitor the time at which the viscosity reached that position and the resulting changes in viscosity. The table below reports the wetout times at each sensor. Note sensor 1 was located at the bottom of the panel and its wetout time is the time when the resin began to flow. Sensors 3, 6 and 9 were at the top of the back stiffener and wetout last.

| Sensor Location   | 1  | 2   | 3   | 4   | 5  | 6   | 7   | 8   | 9   |
|-------------------|----|-----|-----|-----|----|-----|-----|-----|-----|
| Wetout Time (min) | 63 | 104 | 168 | 114 | 97 | 168 | 110 | 100 | 163 |



**Fig. 10** A drawing of the positions of the sensors in the advanced fiber architecture blade stiffened panel. The panel is impregnated with epoxy using vacuum assisted resin infusion from the bottom of the panel

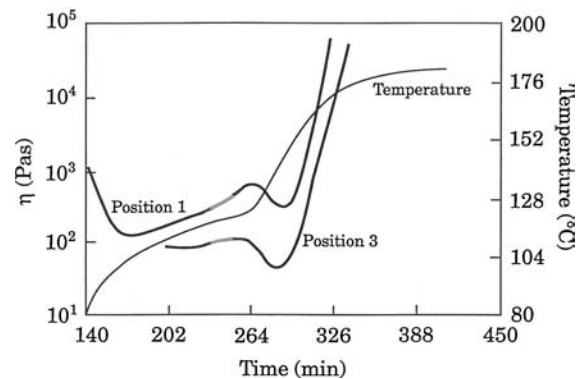
Figure 11 reports the viscosity of the resin underneath the panel at sensor 1 and the viscosity of position 3 after resin reaches this position.

Further details of model predictions and their verification during resin infusion of 3-dimensionally stitched complex fiber preforms have been previously reported. [9–10].

**Automated intelligent closed loop control**

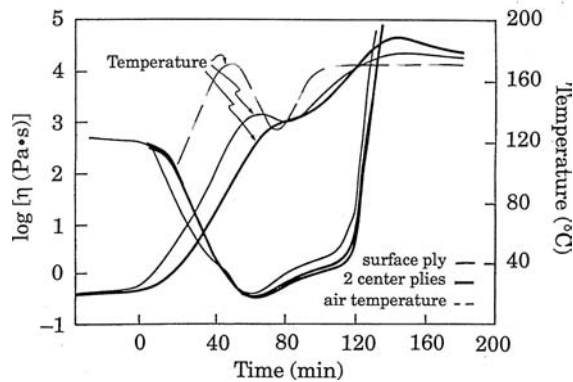
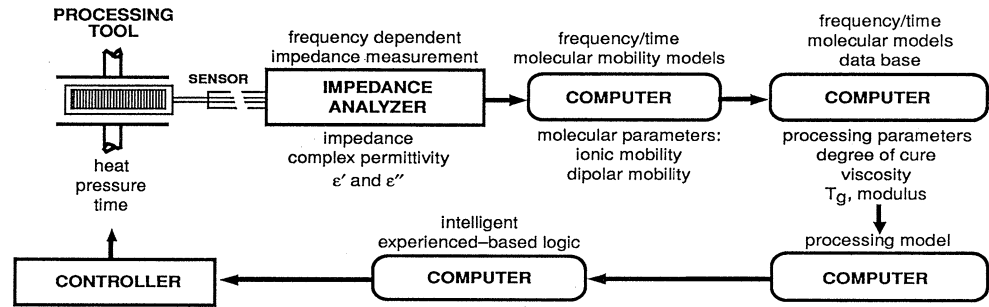
Using models to predict how the cure processing properties should ideally change at each stage of fabrication, sensors can be used to monitor the fabrication process, verify when the appropriate stage has been successfully completed such as complete resin infusion of the graphite perform and then to adjust the temperature and pressure for the next stage, not based on time but rather the actual state of the resin-fiber system. [11–14]

Figure 12 is a schematic of such an intelligent closed loop system. Figure 13 displays the temperature and viscosity during an intelligent automated cure of the one inch thick epoxy graphite panel described earlier. Here fabrication rules were developed based on model predictions and user expertise in which the air temperature increased



**Fig. 11** The sensor measured viscosity of the epoxide at the bottom of the panel, sensor 1, and at position 3 after wetout

**Fig. 12** A schematic of the automated closed loop intelligent sensor controlled system

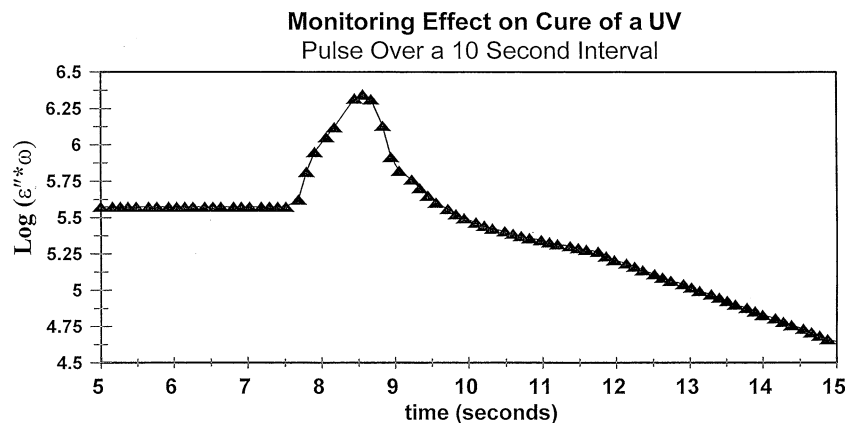


**Fig. 13** The viscosity at various ply positions of a thick laminate when cured using the closed loop intelligent rule based sensor controlled system

and then would be held at 180 °C until the viscosity at the center ply achieved the viscosity at the outer ply. Then the heat was turned off and the exotherm at the center ply increased the reaction advancement and viscosity fairly uniformly throughout the 192 plies. Twenty minutes later, after moving through the viscosity minimum under pressure, the heat was turned on to bring the panel back to 180 °C. The heat was turned off after full cure was achieved as indicated by the sensors.

Based on ultrasonic C-scans a one-inch thick panel free of voids was produced in 180 min versus 240 min using the conventional cure cycle.

**Fig. 14** The dielectric loss multiplied by frequency during rapid cure of a coating after a one-second exposure of UV radiation



## Rapid cure by UV and electron beam radiation

Over the past decade considerable attention has been directed to radiation induced cure as it can be very rapid, more precisely controlled and can reduce many problems associated with thermal cure. Applications include rapid cure of coatings, films and points for uses such as paint on antennas, rapid cure of repair patches on a composite and improved control and speed in filament winding [15–18].

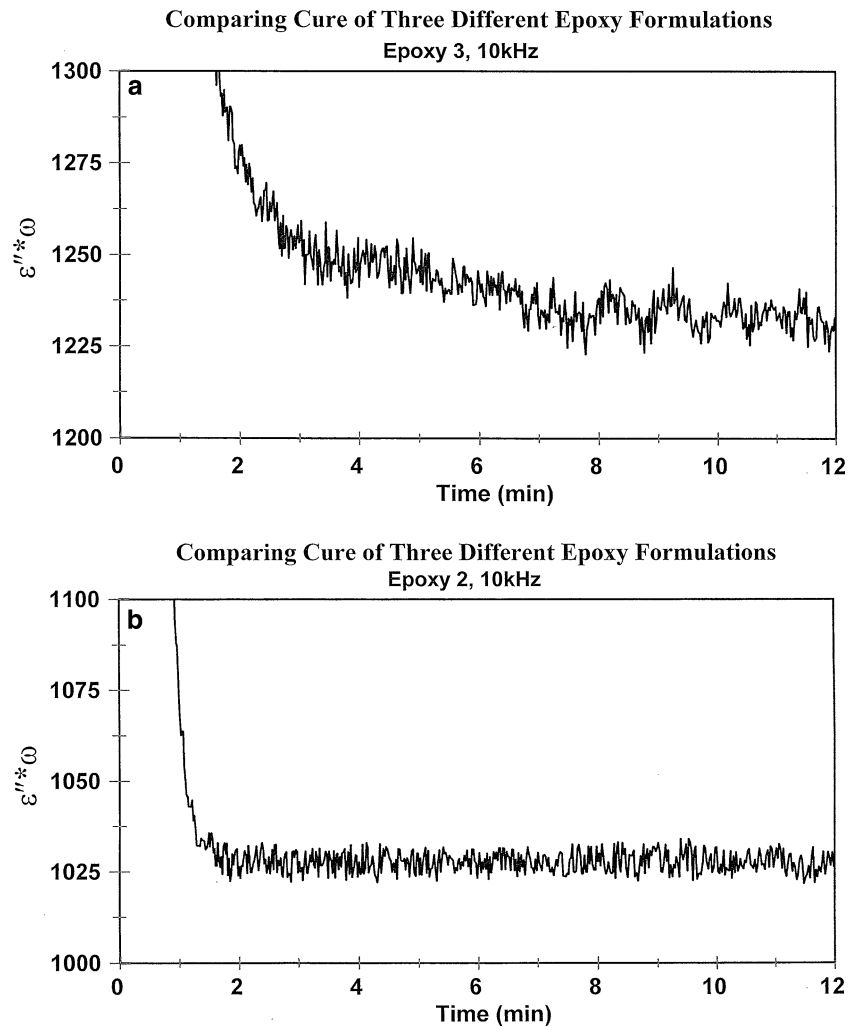
Electric field sensors can be placed at any location in a part and are ideal for monitoring cure of a coating when placed on the substrates surface as they monitor changes in state at the bottom of the coating with one side of the resin exposed to air and the other facing the substrates surface.

Figure 14 displays sensor output during irradiation of a one second UV pulse and the subsequent rate of cure after the irradiation at the 8th second. Approximately 9 measurements were made per second. Figure 15a, b display the sensor's ability to demonstrate that one epoxy formulation reaches full cure in 60 s while the second while appearing to reach full cure in about a minute, actually takes 8 min to achieve full cure.

## Life monitoring

Aging, degradation and reduction in performance properties during use in the field is another application. Here

**Fig. 15** The dielectric loss multiplied by frequency of two different coating formulations to determine which achieves full cure most rapidly after a one-second UV dose



sensors can be embedded in witness coupons exposed along side the actual composite structure to the same fluctuations in the environment during use. Sensors can

**Instrumented Polymer Ageing  
Coupon system**  
SERVICE LIFE MONITORING FOR FLEXIBLE PIPES USING FDEMS



**Fig. 16** A commercially available electric field sensor system for monitoring aging of performance properties subsea of the polymer lining in pipes used to transport crude oil to floating platforms

also be embedded and left in the structure itself during fabrication [19–21]. Figure 16 displays a commercially available sensor system used to monitor aging of the polymer liner in a flexible pipe used to transport oil-gas from the ocean floor to a floating platform.

Degradation generally involves chemical processes which produce changes at the molecular level and which in one sense are the reverse of what happens during cure. Thus, electric field sensors embedded in the material can also detect aging and changes in performance properties in situ during use. As in fabrication, the sensor output needs to be calibrated with changes in mechanical properties or material properties such as degradation due to UV radiation, high temperature, atomic oxygen, or penetration of fuel oil, acid or water. During aging these changes occur much more slowly and are generally much smaller than during fabrication. Thus, monitoring aging requires more precision and sensitivity than in monitoring the state of a part during fabrication.

**Acknowledgements** Thank you to the authors, Justin Doo, Yuemei Zhang and Alfred C. Loos. Support from NASA Langley, the Air Force Edwards California Laboratory, Boeing-McDonnell Douglas Aircraft Company and ICI's Coatings Companies is gratefully appreciated.

## References

1. Kranbuehl D (1997) In: Runt J, Fitzgerald J (eds) Dielectric spectroscopy of polymeric materials, Am Chem Soc., Washington, DC, p 303
2. Kranbuehl D (1991) *Plastics, Rubber, Composite Process* 16:213
3. Poncet S, Boiteaux G, Sautereau H, Seytre G, Rogozinski J, Kranbuehl D (1999) *Polymer* 40:6811
4. Brown JM, Srinivasan S, Ward T, McGrath J, Loos AC, Hood D, Kranbuehl D (1996) *Polymer* 37:1691
5. Kranbuehl D (2000) *Processing of Composites*, Hansor 137
6. Ciriscioli P, Springer G (1990) "Smart Autoclave Cure of Composite Technomic Publishing Co.
7. Kranbuehl D (2002) *Encyclopedia of Smart Materials*, John Wiley, p 456
8. Kranbuehl D (2000) *Processing of Composites*, Hansor 137
9. Kranbuehl D, Loos A (1999) *Resin Transfer Molding for Aerospace Applications*, Chapman Hall, p 412
10. Hasko G, Dexter H, Loos A, Kranbuehl D (1994) *J Adv Mater* 26:9
11. Hart S, Kranbuehl D, Hood D, Loos A, Koury J, Harvey J (1994) *Int SAMPE Symp Proc* 39(1):1641
12. Kranbuehl D, Hood D, Rogozinski J, Limburg W, Loos A, MacRae J, Hammond V (1995) *Int SAMPE Symp. Proc* 40(1)
13. Kranbuehl D, Hood D, Rogozinski J, Barksdale R, Loos A, MacRae D (1995) *Proc ASME Int Mech Eng Congress H1041A* 2:1017
14. Lepene BJ, Long TE, Meyer A, Kranbuehl D (2002) *J Adhesion* 78(4):297
15. Kranbuehl D, Domanski A (2004) *J Coat Technol*, p 48
16. Kranbuehl D, Hood D, Rogozinski J, Meyer A, Neag M (1999) *Prog Org Coat* 881
17. Kranbuehl D, Hood D, Kellam C, Yang J (1996) In: Proudler T (ed) *Am Chem Soc Sym Sev* 648:96
18. Kranbuehl D, Rogozinski J, Meyer A, Hoipkemeier L, Nikolic N (2001) Provder T, Urban M (eds) *Am Chem Soc*, 790:141
19. Kranbuehl D, Newby-Mahler W, Hood D, Cuse S, Reifsnider K, Loos A (1997) In: Chang FK (ed) *Structural Health Monitoring*, Technomic, Penn, p 33
20. Kranbuehl D, Hood D, McCullough L, Eriksen M, Hov E (1994) *Proc. ICC Cont on Inspection of Structural Composites*
21. Kranbuehl D, Hood D, Rogozinski J, Meyer A, Powell E, Higgins C, Davis C, Hoipkemeier L, Ambler C, Elko C, Olukeu N (2000) *Recent Devel Durability Anal Composit*, 413